REPORT DOCUMENTATION PAGE

Form Approved
OMB No. 0704-0188

1. REPORT DATE *(DD-MM-YYYY)*	2. REPORT TYPE	3. DATES COVERED *(From - To)*
26-01-2000	Paper	

4. TITLE AND SUBTITLE

Remarkable AO Resistance of POSS Inorganic/Organic Polymers

5a. CONTRACT NUMBER

5b. GRANT NUMBER

5c. PROGRAM ELEMENT NUMBER

6. AUTHOR(S)

Phillips, S.; Gonzales, R.; Chaffee, K.; Haddad, T. (ERC); Hoflund, G.;

Hsiao, B.; Fu, B.

5d. PROJECT NUMBER
2303

5e. TASK NUMBER
M1A3

5f. WORK UNIT NUMBER

7. PERFORMING ORGANIZATION NAME(S) AND ADDRESS(ES) AND ADDRESS(ES)
Air Force Research Laboratory (AFMC)
AFRL/PRS
5 Pollux Drive
Edwards AFB CA 93524-7048

8. PERFORMING ORGANIZATION REPORT

9. SPONSORING / MONITORING AGENCY NAME(S) AND ADDRESS(ES)

Air Force Research Laboratory (AFMC)
AFRL/PRS
5 Pollux Drive
Edwards AFB CA 93524-7048

10. SPONSOR/MONITOR'S ACRONYM(S)

11. SPONSOR/MONITOR'S NUMBER(S)
AFRL-PR-ED-TP-2000-021

12. DISTRIBUTION / AVAILABILITY STATEMENT
Approved for public release; distribution unlimited.

13. SUPPLEMENTARY NOTES

14. ABSTRACT

15. SUBJECT TERMS

16. SECURITY CLASSIFICATION OF:			17. LIMITATION OF ABSTRACT	18. NUMBER OF PAGES	19a. NAME OF RESPONSIBLE PERSON
a. REPORT	b. ABSTRACT	c. THIS PAGE			Shawn Phillips
Unclassified	Unclassified	Unclassified	A		19b. TELEPHONE NUMBER *(include area code)* (661) 275-5416

Remarkable AO Resistance of POSS Inorganic/Organic Polymers

Shawn H. Phillips, Lt. Rene I. Gonzalez,
Kevin P. Chaffee, Timothy S. Haddad
Edwards Air Force Research Laboratory,
Edwards AFB, CA 93524-7680

Gar B. Hoflund
Department of Chemical Engineering
University of Florida
Gainesville, FL 32611-6005

Benjamin S. Hsiao, Bruce X. Fu
Department of Chemistry
State University of New York at Stony Brook
Stony Brook, NY 11794-3400

ABSTRACT

Polymeric materials offer many advantages for Low Earth Orbit applications including ease of processing and reduced payload-to-orbit costs from the reduction in weight. However, currently applied materials are limited by their severe degradation as a result of atomic oxygen (AO) impingement, vacuum-ultraviolet irradiation and thermal cycling. The Air Force Research Laboratory has dramatically improved polymer properties through the incorporaton of hybrid organic/inorganic POSS (Polyhedral Oligomeric Silsesquioxane). The POSS frameworks are comprised of a three dimensional inorganic core with a 3:2 O-Si ratio, surrounded by tailorable organic groups. POSS incorporation results in increased use and decomposition temperatures, improved mechanical properties, and oxidation resistance. Results of flammability and char motor tests have shown the rapid formation of a ceramic SiO_2 layer, making the hybrid POSS-polymers potential candidates as space resistant materials. This paper reports on the AO resistance of POSS-PDMS and POSS-polyurethanes, with the data obtained using a unique high-purity AO source coupled with *in situ* XPS. Experimental results show the rapid formation of a passivating SiO_2 layer, which is known to be self-annealing in the presence of VUV radiation. Discussions will be centered on the synthesis of the hybrid POSS polymers, AO testing and subsequent material characterization.

KEY WORDS: atomic oxygen, POSS, silsesquioxane, polymer, space

1. INTRODUCTION

Aggressive environments encountered in every space mission have continually challenged the integrity of existing high-performance materials. Reported space environment damage to man-made bodies in orbit is staggering with numerous studies indicating that both radiation (atomic oxygen, vacuum ultraviolet, proton, electron and particle) damage and thermal cycling contribute to material degradation, which drastically reduces the lifetime of the orbiting body. Polymers are very attractive and desirable materials for use in space applications because they could potentially solve many of the weight-based and process-based problems plaguing the space industry. However, polymers are especially susceptible to radiation damage. In particular, the high flux of electromagnetic radiation in earth orbit can decrease the stability of polymers. This is due to their relatively low bond dissociation energies. Table 1 lists the bond dissociation energies for bonds found in commonly used space-qualified polymers Kapton® and FEP Teflon®. With the exception of the CF_2-F bond in FEP Teflon® the energies to break these bonds are very low, < 4.5 eV, the approximate collision energy of atomic oxygen. However, commonly used inorganics tend to have bond dissociation energies larger than those of organic polymers, (Table 1) as well as having an enhanced ability to absorb vacuum ultraviolet radiation.

Table 1. Bond dissociation energies for commonly used space polymers and inorganic materials.

Bond	Dissociation Energy (eV)	λ ([nm])	Material
$-C_6H_4C(=O)-$	3.9	320	Kapton®
C-N	3.2	390	Kapton®
CF_3-CF_3	4.3	290	FEP Teflon®
CF_2-F	5.5	230	FEP Teflon®
Si-O	8.3	150	Nanocomposite
Zr-O	8.1	150	Nanocomposite
Al-O	5.3	230	Nanocomposite

The hybrid polymer research program at the Air Force Research Laboratory at Edwards (AFRL/PRSM) has focused on the incorporation of Si-O containing frameworks into traditional polymers. This research has shown that addition of POSS (POSS = Polyhedral Oligomeric Silsesquioxanes) monomers via copolymerization, grafting, or blending results in numerous property enhancements, including increased modulus and temperature stability, oxidation resistance, and ceramic-layer formation. These enhacements are obtained without adversely affecting the density or processibility of the polymer matrix, which will be discussed. Flammability studies, rocket motor insulation testing, and preliminary atomic oxygen results have shown that upon degradation, the hybrid organic/inorganic nanocomposites form a passivating Si-O layer.

Three primary POSS-polymer architectures (bead, pendant or crosslinker) are available for use in thermoset systems or in copolymerizations as shown in Figure 1. Cooperative efforts by AFRL/PRSM and Hybrid Plastics, LLC have lead to the optimization of condensation reactions of alkyltrichlorosilanes resulting in an economical synthetic route to obtain the starting POSS cages. The synthetic methods to form more than fifty monomers, readily usable in conventional polymerization reactions, have been developed to date (1).

Recent detailed experimental and theoretical (2) results have shown that general property enhancements result from POSS-polymer matrix interactions. Chain-entanglement through associated and knotted-rope diffusion, and the size and mass of the POSS cage (~15 Å, 1000 amu) are all likely to have roles on the physical properties. The fundamental cage size and higher length scale association of the cages produces a structural hierarchy that greatly influences physical properties. For example in the POSS-norbornyl system, increasing the chain length of the noninteractive organic groups by one carbon results in a 30% higher glass transition temperature (T_g), which was shown by transmission electron microscopy to result from POSS entrainment of the polymer network (3).

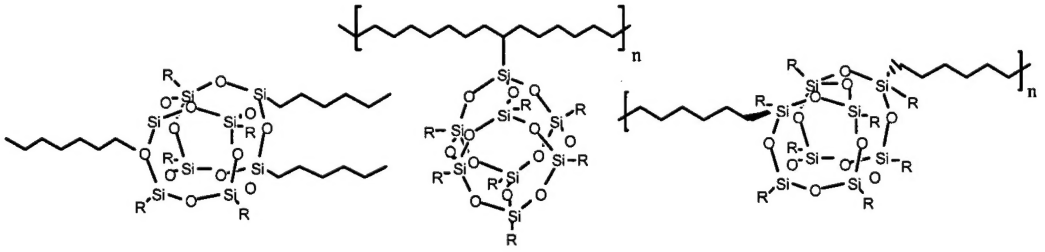

Figure 1 POSS-polymer Structures.

The property improvements obtained by POSS addition, such as increased oxidation resistance and elevated T_g, suggest their effectiveness for space applications including protective coatings, paints, thermal control components and space inflatables. The effect of atomic oxygen (AO) on spacecraft material degradation has been studied on materials exposed in space [STS missions and NASA Long Duration Exposure Facility (LDEF)] (4-7) and in simulation facilities (8-10). In these studies the samples were analyzed by X-ray photoelectron spectroscopy (XPS) but only after exposing the AO-treated samples to air. Recent studies have shown that exposure to air chemically alters the reactive surfaces formed during AO exposure (11,12). Therefore, *in-situ* AO erosion studies of polymers must be performed to avoid artifacts induced by air exposure. For this study, a novel electron stimulated desorption (ESD) atomic oxygen source combined with *in-situ* XPS was used to determine the effect of AO on a new polyurethane containing 60 wt% POSS (POSS-PU) before and after incremental exposures. These results are compared those recently reported for a similar study on a POSS-polydimethylsiloxane (POSS-PDMS) polymer (13).

2. EXPERIMENTAL

2.1 Materials

2.1.1. Preparation of the POSS-PDMS copolymer The POSS siloxane copolymer used in this study, shown in Figure 2, was synthesized using a method similar to that described by Lichtenhan et al. (14,15).

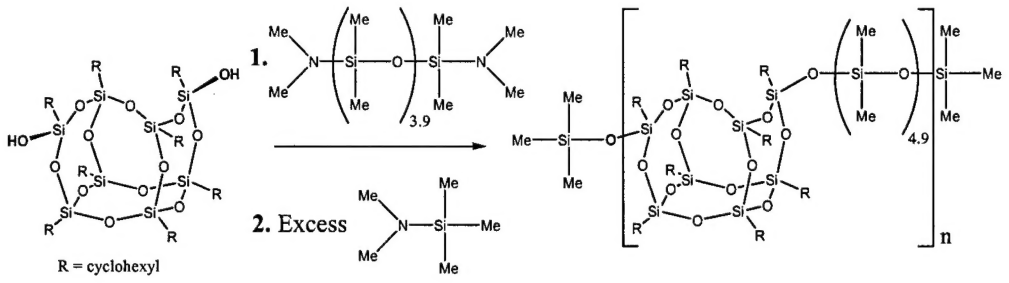

Figure 2 Synthetic scheme for synthesis of the POSS-PDMS copolymer.

2.1.2 Preparation of the 60 wt % POSS-Polyurethane copolymer Polyurethane samples were synthesized by a two-step solution reaction described by Hsiao et al. (16). Diphenylmethane-4,4'-diisocyanate (MDI) and polytetramethylene glycol (PTMG) (Mw=2000) were mixed in a molar ratio of 2:1 and prepolymerized at 80°C for 2 hrs. The prepolymer was dissolved into anhydrous polytetrahydrofuran (PTHF). The prepolymer was then chain extended by addition of POSS-TMP diol at room temperature over 6 hours. The mixture was cooled to 5 °C and 1,4-butanediol (BDO) added drop-wise. The system was warmed to room temperature and after 1 hour the products were precipitated in a 1:1 methanol-water solution, separated by filtration and dried in *vacuo*. All the reactions were carried out under nitrogen.

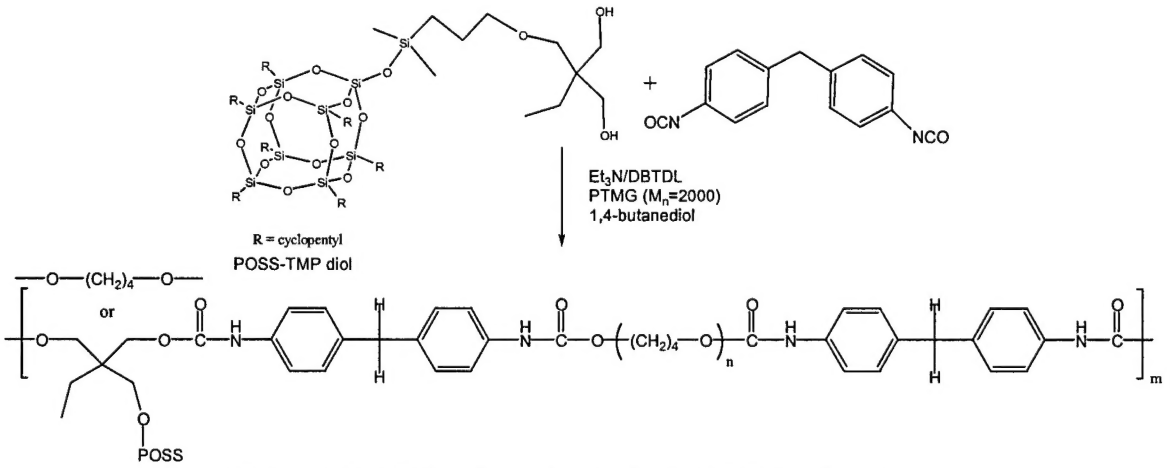

Figure 3 Synthetic scheme for synthesis of POSS-polyurethane.

2.1.3. Preparation of Thin Films by Solvent Casting Thin films of the POSS-PDMS and the 60 wt % POSS-PU were made by solvent casting THF solutions of 5mg / mL concentration of each polymer onto 1 cm x 1 cm aluminum substrates. The films were dried at room temperature for 24 hrs. The aluminum substrates were cleaned with Boraxo^{TM} soap and water, rinsed with deionized water, followed by ultrasonic cleaning in toluene, acetone, trichloroethylene, acetone and ethanol successively.

2.2 Polymer Characterization.

Molecular weights were determined from multi-angle laser light scattering measurements obtained from a DAWN-F detector (Wyatt Technologies) equipped with a gel-permeation chromatography column. Analysis of the POSS-PDMS yielded a number average molecular weight (M_n), mass average molecular weight (M_w) and degree of polymerization of 62,000, 118,000 and 43 respectively. Peak area analysis of the ^{29}Si NMR data gives a degree of polymerization of 38 and shows on average 4.8 $SiOMe_2$ groups per repeat unit. Relevant peaks in the ^{29}Si NMR spectrum are a singlet at 7.2 ppm (Me_3Si endgroups, peak area of 2.0), a multiplet at 21.5 ppm (Me_2Si -O, peak area of 184) and four singlets at 66.39, 68.13, 68.20 and 69.51 ppm (POSS, peak area of 305.6). Analysis of the 60 wt% POSS-PU yielded an M_n and M_w of 62,000 and 110,000 respectively.

2.3 Atomic Oxygen and Vacuum Ultra-Violet Testing and XPS Analysis of Polymers

2.3.1. O-Atom Source Characteristics The ESD source used in this study was developed by Hoflund and Weaver (17), and is commercially available through Atom Sources, Inc. It is ultrahigh vacuum (UHV) compatible, operates with the sample at room temperature, and produces a high-purity, hyperthermal (>1.0 eV), AO flux with an O atom: O^+ ratio of about 10^8. These sources are superior to plasma sources in that they produce primarily ground-state O atoms and operate at UHV pressures (~10^{-9} torr) while producing negligible amounts of other species, including ions, and UV and IR radiation. The operational concept of the hyperthermal oxygen atom generator is shown in Figure 4.

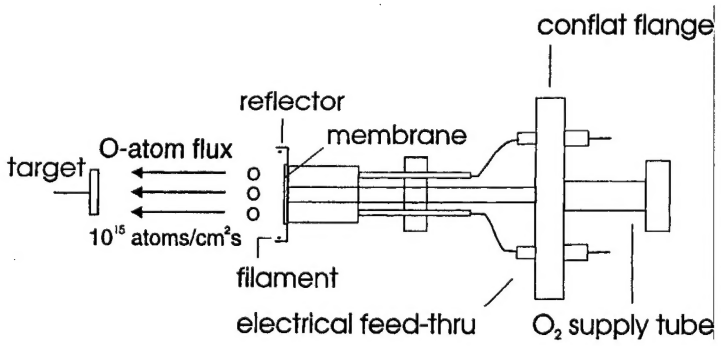

Figure 4 Schematic diagram of the atom source.

Ultrahigh purity molecular O_2 dissociatively adsorbs on a metallic Ag alloy membrane at the high-pressure side and permeates at elevated temperature (~400 °C) to the UHV side. There the adsorbed atoms are struck by a directed flux of primary electrons, which results in ESD of O atoms forming a continuous flux. The O atoms produced by this source have been shown to be hyperthermal, but their energy distribution has not been measured. Corallo et al. (18) have measured the energy distribution of O ions emitted by ESD from a Ag(110) surface and found that this distribution has a maximum at approximately 5.0 eV and a full-width at half maximum of 3.6 eV. This ion energy distribution would set an upper bound for the neutral energy distribution because ESD neutrals are generally believed to be less energetic than ESD ions.

This point has been discussed often in the ESD literature but not actually demonstrated. A mass spectrometer has been used to characterize the flux produced by this ESD source. The ion acceleration potential was set at 0.0 V in these studies. Since calibration studies demonstrated that the ions entering the quadrupole section had to have a minimum kinetic energy of 2.0 eV to reach the detector, the ESD neutrals have a minimum energy of 2.0 eV. Therefore, the hyperthermal AO produced by this ESD source have energies greater than 2.0 eV but less than the maximum of the ion energy distribution.

2.3.2. Surface Characterization Solvent cast POSS-PDMS and 60 wt% POSS-PU films were wiped with isopropanol and inserted into the UHV chamber (base pressure $<10^{-10}$ torr). XPS was performed using a double-pass cylindrical mirror analyzer (DPCMA) (PHI Model 25-270AR) and a Mg Kα X-ray source (PHI Model 04-151). XPS survey spectra were taken in the retarding mode with a pass energy of 50.0 eV. High-resolution XPS spectra were taken with a pass energy of 25.0 eV. Data collection was accomplished using a computer interfaced, digital pulse-counting circuit followed by smoothing with digital-filtering techniques. The sample was tilted 30 deg off the axis of the DPCMA, and the DPCMA accepted electrons emitted into a cone 42.6 ± 6 deg off the DPCMA axis.

XPS spectra were first obtained from the as-entered, solvent-cleaned samples. The samples were then transferred via a magnetically coupled rotary/linear manipulator into the adjoining UHV chamber that houses the ESD AO source. There the surfaces were exposed to the hyperthermal AO flux and re-examined *in-situ* after total exposure times of 2.0, 24.6 (POSS-PDMS), 24.0 (POSS-PU), and 63.0 h. The approximate normal distance between the sample faces and source in this study was 15 cm, at which distance the flux was about 2 x 10^{13} atoms/cm^2-s for the instrument settings used. Substrate temperatures were determined using a chrome-alumel thermocouple attached to the Al substrates. The samples remained at room temperature during the AO exposures. However the sample temperatures did increase to 50 °C during XPS data collection. After the 63.0 h AO exposure, the samples were exposed to air (room temperature ~22 °C and relative humidity ~60%) for 4.8 hrs (POSS-PDMS), 3.3 hrs (POSS-PU) and reexamined using XPS.

3. RESULTS AND DISCUSSION

The XPS survey spectra obtained from a solvent-wiped POSS-PDMS and a 60 wt% POSS-PU surface before and after the 2.0, 24.0 and 63.0 h AO exposures are shown in Figure 5 and Figure 6 a through d, respectively. Spectrum e in Figure 5 and 6 were taken after a 4.8 h and 3.3 h air exposure respectively following the 63.0 h AO treatment. The peak assignments shown in these figures pertain to all five spectra. The predominant peaks in these spectra include the C 1s, O 1s, Si 2p, Si 2s, O 2s and O KVV Auger peaks for the POSS-PDMS sample, as well as the N 1s, Sn 3d and the Na KLL Auger peaks for the POSS-PU. The presence of Sn is attributed to the catalyst system (dibutyltindilaurate) used during urethane synthesis. Na is present in parts per million levels in the reactants used to make the catalyst system and migrates to the surface as a result of AO exposure and affinity for silica. Significant changes in relative peak heights are observed for the C, O, and Si features following the AO exposures. Estimates of the near-surface compositions have been calculated from the peak areas in the survey spectra using published atomic sensitivity factors (19) with the assumption of a laterally homogeneous surface. The

compositions determined in this manner are presented in Tables 2 and 3 for the as-entered, AO-exposed and air-exposed surfaces.

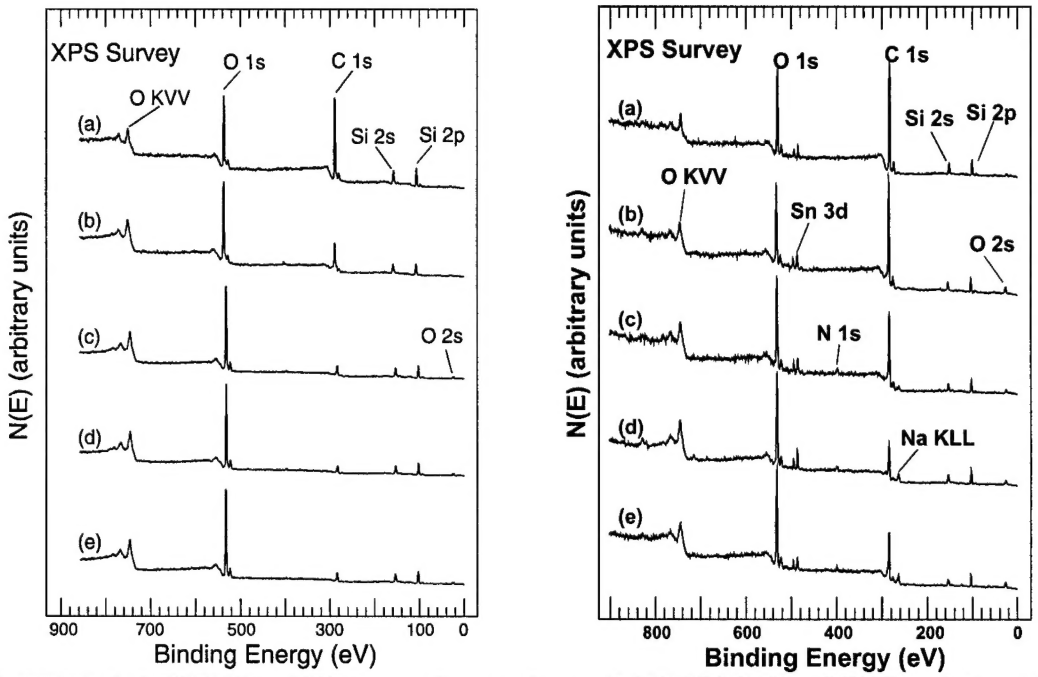

Figure 5 (LEFT) & 6 (RIGHT) XPS Survey Spectra from a POSS-PDMS film (LEFT) and 60 wt% POSS-PU (RIGHT) (a) after insertion into the vacuum system, (b) after a 2.0 h (c) 24.6 h (LEFT), 24 h (RIGHT) and (d) 63.0 h exposure to the hyperthermal AO flux, and (e) 4.8 h (LEFT), 3.3 h (RIGHT) air exposure following the 63.0 h exposure.

XPS probes the near-surface region of the sample and yields a weighted average composition with the atomic layers near the surface being weighted more heavily since these photoemitted electrons have a lower probability of inelastic scattering. The sampling depth is about 30 atomic layers, and about 10% of the signal originates from the outermost atomic layer (20). This near-surface region is nonhomogeneous through depth because the AO reacts with the outermost few atomic layers. Therefore, the region which is affected the greatest by AO also makes the largest contribution to the XPS signal. This fact implies that XPS is an excellent technique for studying AO erosion of spacecraft materials. Even though the distribution functions involving the depth of chemical reactions in the near-surface region and the XPS determination of the weighted average composition of the near-surface region are complex, the compositional values provide a trend which is indicative of the chemical alterations occurring during AO exposure. The compositions were determined using the homogeneous assumption and are shown in Tables 2 and 3 as a function of AO fluence. This trend is supported by the chemical state alterations determined by XPS, which were recently reported for the POSS-PDMS sample (13) and are analogous to the POSS-PU sample discussed below.

Table 2. Near-surface composition determined from XPS data obtained from the as-entered, solvent cleaned, AO and air-exposed POSS-PDMS sample

Surface	AO Fluence	Composition, atomic %			atom ratio
Sample Treatment	O/cm^2	O	C	Si	O/Si
As entered, solvent cleaned	---	18.5	65.0	16.6	1.11
2.0 h AO exposure	1.44×10^{17}	33.8	48.4	17.8	1.90
24.6 h AO exposure	1.77×10^{18}	49.1	22.1	28.8	1.70
63.0.0 h AO exposure	4.53×10^{18}	55.7	16.3	28.0	1.99
4.8 h air exposure following the 63.0 h AO exposure	4.53×10^{18}	52.8	19.5	27.7	1.91

Table 3. Near-surface composition determined from XPS data obtained from the as-entered, solvent cleaned, AO and air-exposed 60 wt % POSS-Polyurethane sample

Surface	AO Fluence	Composition, atomic %						atom ratio
Sample Treatment	O/cm^2	O	C	Si	Sn	Na	N	O/Si
As entered, solvent cleaned	---	18.2	70.1	11.3	0.4	-	-	1.61
2.0-h O-atom exposure	1.44×10^{17}	17.5	70.2	11.2	0.7	0.4	-	1.56
24.0-h O-atom exposure	1.77×10^{18}	23.7	58.2	13.2	0.9	1.4	2.6	1.79
63.0.0-h O-atom exposure	4.53×10^{18}	35.3	37.3	20.4	1.3	3.0	2.7	1.73
3.3-h air exposure following 63.0-h O-AO exposure	4.53×10^{18}	31.6	48.5	14.6	1.0	2.7	1.6	2.16

Atomic oxygen exposure results in an increase in the O-to-Si atomic ratio from an initial 1.11 for the as-entered sample POSS-PDMS sample to 1.99 after the 63.0 h O-atom exposure. A similar increase from an initial 1.61 to 1.73 is observed in Fig 6. for the POSS-PU sample. This behavior indicates that complex chemical reactions occur during AO exposure. Exposure to air resulted for both the POSS-PDMS sample resulted in no significant change in the O-to-Si ratio, however a subsequent increase to 2.16 was observed in the POSS-PU. These changes in the O-to-Si atomic ratio resulting from exposure to the AO flux indicate the formation of SiO_2 and are consistent with the high-resolution spectra that follow. A large reduction in the C 1s peak is observed as a result of the incremental exposures to the AO flux in both samples. The near-surface C concentration decreases from 65.0 at% for the as-entered POSS-PDMS sample to 16.3 at% after the 63.0 h exposure. The POSS-PU carbon content decreases from 70.1 to 37.3 at%. This decrease is due to reaction of C in the near-surface region with O to form CO and CO_2. In both cases, an increase in the carbon content is observed after exposure to air and is probably due to the adsorption of C-containing molecules (e.g., hydrocarbons) from the air. Hydrogen would also react with the AO to form water, which would desorb from the surface of the sample.

High-resolution XPS C 1s, O 1s and Si 2p obtained from the as-received, solvent-wiped POSS-PU surface before and after the 2.0, 24.0 and 63.0 h AO exposures are shown in spectra a-d of Figs. 7, 8 and 9, respectively. Spectrum e was obtained after the 3.3 h air exposure following the 63.0 hr AO exposure. Variations in peak shapes and positions are observed between the nonexposed, AO-exposed, and air-exposed surfaces, indicating that the chemical species distribution is altered by exposure to the AO flux and then to air.

The C 1s peak, shown in Figure 7a, is broad and centered at 285.0 eV, indicating that the predominant form of carbon present for the as-entered POSS-PU sample is aliphatic, located on the hard and soft segments of the polymer chain and on the cyclopentyl groups of the POSS cages (21). In spectra b-d, the C 1s peak becomes broader displaying visible shoulders with increasing exposure to the O-atom flux. A shoulder due to aromatic carbon is present in these spectra at 284.7 eV. Small shoulders are also visible on the high BE side of the C 1s peak in spectra b, c and d. These are due to species such as alcohols, formaldahydes (BE ~286.0 to 287.7 eV) and organic acids (BE ~287.5 eV), which form by reaction with the AO flux. These changes coincide with a decrease in the total carbon concentration in the near surface region from 70.1 to 37.3 at%. A dramatic reduction in the carbon concentration after AO exposure was also seen in the POSS-PDMS sample studied previously. Exposure to air (spectrum e) produces an 11% increase in C near 285.0 eV indicating adsorption of hydrocarbons from the air at reactive surface sites produced during the AO exposure. A similar observation was also noted for the POSS-PDMS sample (13).

The O 1s spectra obtained from the as-entered POSS-PU sample is shown in Figure 8 (spectrum a). This peak is broad and centered at 531.9 eV. The predominant form of oxygen present for the as-entered sample corresponds to the carbonyl in the urethane segment (531.9 eV) of the polymer and the oxygen present in the POSS cages (532.0 eV). Initially, the oxygen contribution is reduced from 18.2 to 17.5 at% after a 2.0 hr exposure. Spectrum b shows this decrease to coincide with the O 1s peak shifting to a higher BE and thus decreasing the contribution from the urethane segment and the oxygen in the POSS cages. This reduction is consistent with the production and subsequent desorption of CO_2. After the 24.0-h exposure, the near surface O content increases to 23.7 at% and the predominant peak featured in spectra c corresponds to silica. This feature becomes more prominent with the 63.0 h exposure as the surface O content increases to 35.3 at%, and is consistent with the formation of a SiO_2 surface. Exposure to air results in a small 3.7 at% decrease in the surface O content as the reactive surface adsorbs hydrocarbons from the air.

The Si 2p peaks obtained from the POSS-PU sample after the various treatments are shown in Figure 9. The Si 2p peak for the as-entered sample (spectrum a) is broad indicating the presence of several chemical states of silicon. This peak is centered at a BE of 102.7 eV which corresponds to $RSiO_{1.5}$ in the POSS cage. However, spectra b, c and d reveal the formation of a SiO_2 layer with incremental exposures to the O-atom flux. The fact that little difference is observed in the spectra obtained after the 24.0 h and 63.0 h exposures indicates that this silica layer forms a protective barrier on the surface which prevents further degradation of the polymer with longer exposure to the O-atom flux. The significant compositional changes observed indicate that most of the near-surface region examined by XPS is altered by the AO exposure. The chemical reactions that form CO_2 and H_2O are exothermic so the local surface temperature may be relatively high. This and the fact that the AO induces a chemically induced driving force results in diffusion of subsurface C and H to the surface where they react with the AO. This mechanism is responsible for the subsurface compositional alterations observed using XPS. Again, these findings are consistent with those observed for the POSS-PDMS sample (13).

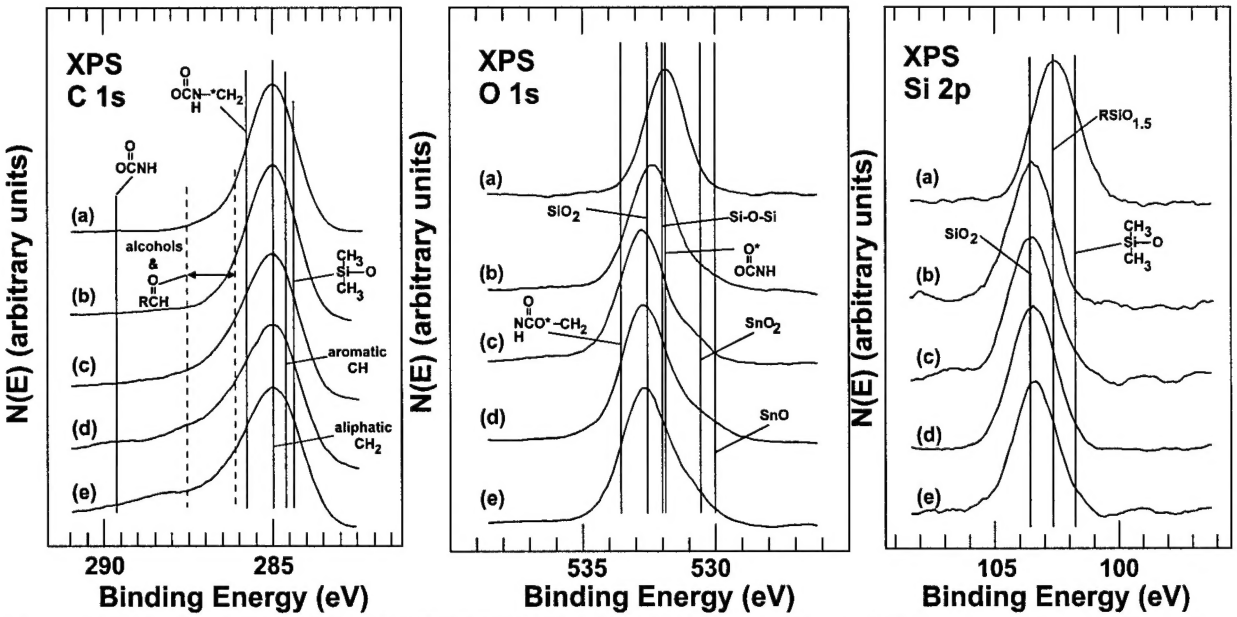

Figure 7 (LEFT), 8(CENTER), 9(RIGHT)XPS High Resulution C1s, O1s and Si 2p spectra from a 60 wt% POSS-polyurethane (a) after insertion into the vacuum system, (b) after a 2.0 h (c) 24.0 h and (d) 63.0 h exposure to the hyperthermal AO flux, and (e) 3.3 h air exposure following the 63.0 h exposure.

4. CONCLUSIONS

Hybrid inorganic/organic polymers containing POSS monomers were synthesized, characterized and tested for atomic oxygen resistance. Samples were placed in a specialized AO source, with the ability to perform *in-situ* XPS analysis. For both the POSS-polydimethylsiloxane and POSS-polyurethane systems a passivating SiO_2 layer formed, resulting from the AO-induced degradation of the organic components and subsequent oxidation of the POSS framework. Changing the composition of the backbone of the polymer system from entirely inorganic (POSS-PDMS) to an inorganic/organic hybrid (POSS-PU) does not adversely affect the formation of the SiO_2 layer. Furthermore, the resulting ceramic SiO_2 layer serves to rigidize the elastomeric materials and prevent further degradation of the virgin polymer. The promising results contained herein when combined with the numerous property enhancements previously reported for POSS incorporation into traditional polymer systems makes their use an attractive alternative to filler or coating systems, when applied to space-based material applications. Future work will focus on studying the physical and mechanical properties of the POSS-polymers after radiation exposure.

5. ACKNOWLEDGMENTS

The authors would like to thank the Air Force Office of Scientific Research Entrepreneurial Research Program (AFOSR/ER) for financial support. In addition the authors would like to thank Lt. Derek Lincoln for allowing the reproduction of Table 1, and Rusty Blanski for technical assistance.

6. REFERENCES

1. U.S. Pat. 5,942,638 (August 24, 1999) Lichtenhan, J. D., Schwab J. J., Feher, F. J., Soulivong, D. (to the United States of America). (b) U.S. Pat. 5,484,867 (January 16, 1996) Lichtenhan, J.D., Gilman, J.W., Feher, F.J. (to the University of Dayton, Regents of the University of California, and United State of America).
2. Farmer, B.L.; Bharadwaj, R.K. accepted for publication in Polymer.
3. Mather, P.T.; Jeon, H.G.; Romo-Uribe, A.; Haddad, T.S.; Lichtenhan, J.D., Macromolecules **32** 1194-1203 (1999).
4. Koontz, S. L., Leger, L. J., Visentine, J. T., Hunton, D. E. , Cross, J. B., and Hakes, C. L., Journal of Spacecraft and Rockets, **32** (3), 483-495 (1995).
5. Reddy, M. R., Journal of Materials Science, **30**, (2), 281-307 (1995).
6. de Groh, K. K., and Banks, B. A., Journal of Spacecraft and Rockets, **31** (4) 656-664, (1994).
7. Banks, B. A., Rutledge, S. K., de Groh, K.K., Mirtich, M. J. Gebauer. L., Olle, R., and Hill, C. M., Proceedings of the 5th International Symposium on Materials in a Space Environment, Cannes-Madelieu, France, 1991, p. 137.
8. Tennyson, R.C., Canadian Journal of Physics, **69** (9), 1190-1208 (1991).
9. Cazaubon, B., Paillous, A., Siffre, J., and Thomas, R., Journal of Spacecraft and Rockets, **33** (6), 870-876 (1996).
10. de Groh, K. K., Terlep, J. A., and Dever, T. M., "Atomic Oxygen Durability of Solar Concentrator Materials for Space Station Freedom," NASA TM-105378, September 1990.
11. Grossman, E., Lifshitz, Y., Wolan, J. T., Mount, C. K., and Hoflund, G. B., Journal of Spacecraft and Rockets, **36** (1), 75-78 (1999).
12. Wolan, J. T., and Hoflund, G. B., Journal of Vacuum Science and Technology A, **17**, (2), 662-664 (1999).

13. Gonzalez, R.I., Phillips, S.H., Hoflund, G.B., accepted for publication in Journal of Spacecraft and Rockets.

14. Lichtenhan, J. D., Vu, N. Q., Carter, J.A., Gilman, J. W., and Feher, F. J., Macromolecules, **26** (8), 2141-2142 (1993).

15. Gilman, J. W., Schlitzer, D. S., and Lichtenhan, J. D., Journal of Applied Polymer Science, **60** (4), 591-596 (1996).

16. Hsiao, B. S., Fu, B. X., White, H., Rafailovich, M., Mather, P. T., Jeon, H. G., Phillips, S. H., Lichtenhan, J. D., and Schwab, J. J., accepted for publication at the 219th National Meeting of the American Chemical society, San Fransico, CA, 2000.

17. Hoflund, G. B., and Weaver, J. F., Measurement Science and Technology, 5 (3), 201-205 (1994)

18. Corallo, G. R., Hoflund, G. B., and Outlaw, R. A., Surface and Interface Analysis, **12**, December, 1988, pp. 185-190.

19. Wagner, C. D., Riggs, W. M., Davis, L. E., Moulder, J. F., and Muilenberg, G. E., Eds., Handbook of X-ray Photoelectron Spectroscopy, Perkin-Elmer Corp., Eden Prairie, MN, 1979.

20. Hoflund, G.B., Handbook of Surface and Interface Analysis: Methods in Problem Solving, Rivière, J. C., and Myhra, S., Eds., Marcel Dekker, Inc., New York, NY, 1998, pp. 57-158.

21. Beamson, G., and Briggs, D., High Resolution XPS of Organic Polymers: The Scienta ESCA300 Database, Wiley, Chichester, England, UK, 1992, pp. 268-269.